The phosphoproteome of Human Jurkat T cell clones upon costimulation with anti-CD3/anti-CD28 antibodies

Tien Dung Nguyen [1,2], Montserrat Carrascal [1], Oriol Vidal-Cortes[1], Oscar Gallardo[1], Vanessa Casas[1], Marina Gay[1#], Van Chi Phan[2], Joaquin Abian [1,&]

[1]CSIC/UAB Proteomics Laboratory, IIBB-CSIC, Barcelona, Spain

[2]Protein Biochemistry Laboratory, IBT-VAST, Hanoi, Vietnam

[#] Current position: Mass Spectrometry Unit, IRB, Barcelona, Spain

[&]Correspondence: Dr. Joaquin Abian, CSIC/UAB Proteomics Laboratory

E-mail: joaquim.abian.csic@uab.cat

Abstract

Phosphorylation is a reversible post-translational modification, playing a vital role in protein function. In T cells, protein phosphorylation is the key mechanism regulating T cell receptor – driven signaling pathways. In order to gain insights into the phosphoproteome evolution of T cell activation, we performed a large-scale quantitative phosphoproteomics study of Jurkat E6.1 (wild type) and Jurkat gamma1 (Phospholipase gamma1 null) cell clones upon costimulation with anti-CD3 and anti-CD28 antibodies at times ranging from 15 min to as long as 120 min. In total, we identified 5585 phosphopeptides belonging to 2008 phosphoproteins from both cell clones. We detected 130 and 114 novel phosphopeptides in Jurkat E6.1 and Jurkat gamma1 clones, respectively. A significantly lower number of proteins containing regulated phosphorylation sites were identified in Jurkat gamma1 in comparison to Jurkat E6.1, reflecting the vital role of Phospholipase gamma1 in T cell signaling. Several new phosphorylation sites from lymphocyte-specific protein tyrosine kinase (Lck) were identified. Of these, serine-121 showed significant changes in JE6.1 while only small changes in the Jgamma1 clone. Our data may contribute to the current human T cell phosphoproteome and provide a better understanding on T cell receptor signaling. Data are available via ProteomeXchange with identifier PXD002871.

Key words: *Phosphorylation, Jurkat T cells, CD3/CD28 costimulation, phospholipase C gamma 1, quantitative phosphoproteomics.*

1. Introduction

Phosphorylation is one of the most frequent PTMs and plays a vital role in the function of proteins. Phosphorylation and dephosphorylation events turn protein enzymes on/off, thereby altering various cellular processes including T cell receptor (TCR) - driven signaling pathways. In T cells, TCR stimulation leads to a series of cellular signals which are mainly regulated by phosphorylation events catalyzed by protein kinases. Engagement of the TCR-CD3 complex changes the structure of intracellular CD3 subunits and facilitates their phosphorylation by lymphocyte-specific protein tyrosine kinase (Lck) [1, 2]. This phosphorylation of the CD3 chains initiates the early TCR signals, including the phosphorylation of zeta-chain-associated protein kinase 70 (ZAP-70) and the formation of a complex between the linker for activation of T cell (LAT) and the SH2 domain-containing leukocyte protein of 76 kDa (SLP-76) [3]. These early signals then activate phospholipase C gamma 1 (PLCγ1), an important enzyme that catalyzes the hydrolysis of phosphatidylinositol bisphosphate (PIP2) to diacylglycerol (DAG) and inositol trisphosphate (IP3) [3, 4]. DAG and IP3 aid the signal transduction to the nucleus by activating or enhancing several transcriptional factors such as the nuclear factor of activated T cells (NFAT), leading to cytokine secretion. The stimulation of the TCR also regulates actin and cytoskeleton remodeling and causes changes in the immunological synapse [5, 6].

The study of cell signaling concentrates on the phosphorylation/dephosphorylation of proteins or kinases participating in various signal transduction pathways. Biological studies using traditional biochemical and immunological techniques often focus only on individual parts of cell signaling pathways and are unable to study new phosphorylation sites (P-sites) if no antibodies are available [6, 7]. Over recent years, the development of phosphoproteomics quantitative approaches for large-scale and systematic analysis of cell signaling, including TCR signaling, has been improved [8-12]. Jurkat cells, including both the wild type and mutant clones, have been widely used for studying T cell signaling in humans [13]. Different T cell signaling studies using Jurkat cells aimed to reveal the phosphorylation dynamics upon TCR/CD3 stimulation [10], phorbol 12-myristate 13-acetate (PMA) and ionomycin activation [14], and combination of TCR/CD3 stimulation with other stimuli such as anti-CD28 or anti-CD4 antibodies [8, 9, 12]. Furthermore, phosphoproteomics studies on TCR signaling attempted to elucidate the effects of certain proteins of the TCR signaling network such as ZAP-70 [12], SLP-76 [8], and LAT [15] on the phosphorylation profile of T cells upon TCR stimulation (CD3 alone or CD3/CD28 costimulation) using available mutant Jurkat T cell clones. These quantitative phosphoproteomics studies produced big datasets of regulated P-sites in response to T cell activation and started out a new strategy using MS-based quantitative methods for systematic cell signaling studies.

This work presents a large-scale quantitative phosphoproteomics study of human Jurkat T cells, including the Jurkat E6.1 (JE6.1 – wild type) and the Jurkat gamma1 (Jgamma1 – PLCγ1 null) clones upon costimulation with anti-CD3/anti-CD28 antibodies. Our aims were to broaden current knowledge on the human Jurkat T cell

phosphoproteome and to evaluate the effects of PLCγ1 on the phosphorylation dynamics of stimulated T cells for a better understanding of TCR signaling. In total, we detected 5585 phosphopeptides corresponding to 2008 phosphoproteins from both cell clones. The significantly lower phosphorylation changes in Jgamma1 may imply the vital role of PLCγ1 on TCR signaling pathways. Interestingly, we detected several novel high confidence P-sites from Lck in response to TCR costimulation, of which serine-121 is among the most remarkable.

2. Materials and methods

2.1. Cell culture and activation

JE6.1 and Jgamma1 cells were obtained from the American Type Culture Collection (Manassas, VA, USA) and cultured according to their guidelines. Previously to activation, cells were incubated in serum-free RPMI-1640 medium at a density of 3×10^6 cells/mL for 6 h. Afterwards, cells were washed and reconstituted at a density of 2.5×10^7 cells/mL in ice-cold serum-free RPMI-1640 medium. For each time point, 2.5×10^7 cells were treated with anti-CD3 (clone OKT3, eBiosciences) and anti-CD28 (clone CD28.2, eBioscience) monoclonal antibodies, at a concentration of 5 µg/mL of each antibody, for 30 min at 4 ^{o}C. After such time, the activation was initiated by collecting and resuspending cells in serum-free RPMI-1640 medium at 37 ^{o}C containing 8.5 µg/mL of goat anti-mouse polyclonal IgG antibody (Invitrogen, Camarillo, CA, USA). Cell density for activation was of 2.5×10^7 cells/mL. Activation was stopped at assigned time points (15, 30, 60, 120 and 1440 min) by diluting cell cultures with 10-fold excess of ice-cold PBS. The cell culture without antibody treatment (0 min) was used as the control.

2.2. Protein extraction and digestion

Cell pellets were suspended in lysis buffer (4% (w/v) SDS, 100 mM Tris/HCl, pH 7.6, 0.1 M DTT) and incubated at 95 ^{o}C for 5 min. To allow for complete cell disruption, the cell extract was sonicated 5 times for 5 s (Sonic Vibracell TM). The cell debris was removed by centrifugation at 16000×g for 20 min at 13 ^{o}C. Protein concentration measurement was performed with the Bradford Protein Assay (Bio-Rad, CA, USA). Five biological replicates from each clone were processed.

Protein was digested with Sequencing Grade Modified Trypsin (Promega, Madison, WI, USA) using the FASP (Filter Aided Sample Preparation) digestion protocol [16]. Briefly, 80 µg of protein corresponding to each time point were loaded to a 10-kDa Amicon Ultra-0.5 centrifugal filter (Millipore, Watford, UK). The protein mixture was washed three times by adding 200 µl of UA buffer (8 M Urea, 0.1 M Tris/HCl pH 8.5) to the filter and centrifuging at 14000×g for 10 min at 13 ^{o}C. Next, proteins were alkylated with 100 µl of alkylation buffer (0.05M IAA, 8M Urea, 0.1 M Tris/HCl pH

8.5) in the dark for 20 min at 25 ^{o}C. Subsequently, the protein extract was washed three times with 100 µl of UA buffer and three times with 100 µl of 200 mM triethylammonium bicarbonate (TEAB). Trypsin digestion was performed at 37 °C for 18 h using an enzyme-to-protein ratio of 5:100. Tryptic peptides were eluted by the addition of 3×100 µl of 200 mM TEAB followed by a centrifugation at 14000×g for 15 min at 13 ^{o}C.

2.3. Peptide labeling by isobaric tandem mass tag

Each tryptic peptide mixture obtained from 80 µg of protein extract was labeled with tandem mass tags (TMT) (Thermo Scientific, Rockford, IL, USA) based on the standard procedure. In short, the tryptic peptide mixtures were evaporated to final volumes of about 60 µl. Each TMT reagent was dissolved in 41 µl of LC/MS-grade ACN (Sigma-Aldrich) and added to the corresponding peptide mixture for labeling. After one hour, the labeling reaction was stopped by adding 8 µl of 5% hydroxylamine. Six labeled peptide mixtures were combined in a low-bind 1.5 mL Eppendorf tube, evaporated, and desalted using a C18 SPE cartridge (3 mL, 15 mg, Agilent Technologies, USA) before separation by Strong Cation Exchange (SCX) chromatography.

2.4. Separation of peptides by Strong cation exchange chromatography

Peptide separation by SCX chromatography was performed on an Agilent 1100 HPLC system (Agilent Technologies, Waldbronn, Germany) using a Polysulfoethyl A TM, 50×2.1 mm, 5 µm, 200 Å column. Peptides were suspended in 200 µl of SCX buffer A (30% ACN, 0.1% formic acid) and loaded onto the column at 200 µl/min of 100% SCX buffer A. Bound peptides were eluted by linear gradient of SCX buffer B (30% ACN, 0.1% formic acid, 500 mM NH_4Cl) from 0 to 25% in 38 min and then to 100% in 20 min. For each injection, samples were separated and collected in 6 final fractions (Figure S1). Each fraction was cleaned up by solid phase extraction before the subsequent phosphopeptide enrichment experiments.

2.5. Phosphopeptide enrichment

Enrichment of phosphopeptides by sequential Immobilized Metal Ion Affinity chromatography (IMAC) and Titanium dioxide (TiO_2) chromatography was carried out according to previous studies [17, 18]. Briefly, the IMAC resin (Phos-Select iron affinity gel, Sigma, St.Louis, MO) was washed three times and added to each peptide extract. The mixtures were incubated for 90 min at 20 °C with end-to-end rotation in a low-bind 0.5 mL Eppendorf tube. Afterwards, samples were transferred to a Mobicol mini-column (MoBiTec, Germany) and washed three times with 200 µl of 250 mM Acetic acid /30% acetonitrile. Phosphopeptides were eluted with 3×50 µl of 0.5% NH_4OH into a 1.5 mL Eppendorf tube containing 20 µl of 10% formic acid. The non-retained fraction was evaporated and resuspended

in 50 µl of 1 M glycolic acid, 5% TFA, 80% acetonitrile for the subsequent TiO_2 phosphopeptide enrichment. The TiO_2 mini-column was prepared by loading TiO_2 slurry (Titansphere, GL Sciences, Japan) onto a GelLoader Tip as previously described [19]. This column was equilibrated with 50 µl of 1 M glycolic acid, 5% TFA, 80% acetonitrile. The sample was loaded onto the column using a syringe; then, the column was washed sequentially with 10 µl of 1 M glycolic acid, 5% TFA, 80% acetonitrile, then 20 µl of 80% acetonitrile, 1% TFA and, finally, 5 µl of water. Bound phosphopeptides were eluted with 20 µl of 0.5% NH_4OH followed by 5 µl of 30% acetonitrile. Each eluate was then acidified with 2 µl of formic acid.

2.6. LC-MS^n Analysis

All IMAC and TiO_2 phosphopeptide fractions were analyzed separately by LC-MS^n using an LTQ-Orbitrap XL instrument equipped with a nanoESI ion source (Proxeon, Odense, Denmark). Samples were evaporated to dryness and redissolved in 20 µl of 1% formic acid and 5% MeOH. The HPLC system was composed of an Agilent 1200 capillary nano pump, a binary pump, a thermostated microinjector and a micro switch valve. Separation was carried out using a C18 pre-concentration cartridge (Agilent Technologies) connected to a 15 cm-long 100 µm i.d. C18 column (Nikkyo Technos Co, Japan). Separation was done at 0.4 µl/min using a linear ACN gradient from 0 to 40% in 180 min (solvent A: 0.1% formic acid, solvent B: acetonitrile 0.1% formic acid). The LTQ-Orbitrap instrument was set up in the positive ion mode with a spray voltage of 1.8 kV. The scan range of each full MS was m/z 400-2000. The spectrometric analysis was performed in an automatic data dependent mode. A full scan followed of 1 HCD and 1 CID MS/MS for the 3 most abundant signals were acquired. A subsequent MS^3 scan was performed when a neutral loss of -98, -49, or -32.7 m/z (loss of H_3PO_4 for the +1, +2, and +3 charged ions, respectively) was detected in the CID MS/MS among the 5 most intense ions. Dynamic exclusion was set to 1 with a time window of 45 s to minimize the redundant selection of precursor ions.

Combination of CID and HCD information for peptide identification and quantitation, respectively, provides an efficient method for quantitative shotgun proteomics [20]. Due to the rich sequence information offered by the CID spectra, CID is preferred for peptide identification to HCD in the Orbitrap XL. CID spectra, however, do not usually contain information on the low-mass reporter ions due to the ion trap scan limitations. Contrarily, the higher fragmentation energy of HCD and the absence of lower-mass limits make this method optimal for monitoring reporter ions.

2.7. Database search and quantitative analysis

Database search was carried out using multiple search engines including SEQUEST (Bioworks v3.3, ThermoFisher, San Jose, CA) [21], OMSSA (version 2.1.4)[22], and EasyProt [23]. The database search workflow was as previously

described [24, 25]. In brief, Thermo RAW files were processed using the EasierMgf software, which generates separate files for the MS/MS and MS^3 data, respectively. At the same time, EasierMgf combines the low mass range data from each HCD MS/MS spectrum with the corresponding CID data obtained for the same precursor in the scan cycle into single MS/MS and MS^3 spectra. These MGF files containing hybrid HCD-extended MS/MS and MS^3 CID spectra, respectively, were used as input for the different search engines. Each search engine was run against the Human Swiss-Prot database (Human Swiss-Prot, release 4-11) using the target-decoy strategy [26]. Database searches for MS^2 and MS^3 were performed separately. MS^2 searches were performed with the following parameters: parent tolerance, 20 ppm; fragment tolerance, 0.8 Da; enzyme, trypsin; missed cleavages, 1; fixed modifications, TMTsixplex (N-terminal, K), carbamidomethyl (C); variable modifications, oxidation (M), phosphorylation (S, T, Y). For the MS^3 searches, the setup parameters included: parent tolerance, 2 Da; fragment tolerance, 0.8 Da; enzyme, trypsin; fixed modifications, TMTsixplex (N-terminal, K), carbamidomethyl (C); variable modifications, oxidation (M), phosphorylation (S, T, Y), dehydration (S, T). The results from the different search engines were combined and filtered using the Integrator software. Only those hits detected from at least two search engines were considered as positive identifications [25]. When a peptide assigned to 2 or more proteins the first accession number in our data was considered in following discussions. The mass spectrometry proteomics data have been deposited to the ProteomeXchange Consortium [27] via the PRIDE partner repository with the dataset identifier PXD002871.

The location of P-sites was evaluated according to the Q-Ascore algorithm by using the Integrator software [25, 28]. P-sites with Q-Ascore≥19 were considered of high confidence. To describe our collections of non-redundant identifications, except when indicated, phosphopeptides with different assignation of the phosphate position were counted separately irrespective of their Q-Ascore value.

Quantitative information of the peptides detected either from the MS/MS or MS^3 fragmentation data was extracted from the HCD MS^2 data already embedded in these hybrid HCD/CID spectra by EasierMgf. When a peptide was identified by both MS^2 and MS^3 spectra, only MS^2 spectra was considered for quantitation. DanteR [29] was used for relative quantification and statistical analysis of TMT-labeled peptides. All scans with signals for at least one reporter ion were considered for quantification. Before DanteR analysis, intensity data was normalized using the median of non-phosphorylated peptides for each reporter ion. DanteR ANOVA was performed at peptide level, with a requirement of at least two measurements, by comparing treated versus control peptides using a linear model. Peptides were ordered using median and minimum number of peptides was set to 1 and maximum to 1000. Finally, p-values were adjusted by using the Benjamini & Hochberg False Discovery Rate (FDR) correction. Regulated

peptides were determined using an adjusted p-value cutoff of 0.05 and a fold change lower than 0.67 (down) or higher than 1.5 (up).

2.8. Biological analysis

Phosphorylation Motif Analysis – The motifs of the regulated P-sites were obtained using the Motif-X algorithm using the following parameters: foreground format, MS/MS; Extend, IPI Human proteome; central characters, S or T; width, 13; background, IPI Human proteome. Occurrences and Significance parameters were set depending of the collection foreground size (see Figure S2). The other parameters were set following the Motif-X algorithm's default profile [30].

KEGG pathway analysis – KEGG pathway analysis – Proteins containing regulated P-sites were mapped to the KEGG pathways using DAVID Bioinformatics Resources 6.7 (http://david.abcc.ncifcrf.gov) [31] and the whole Homo sapiens genome as background.

2.9. Western blot analysis of Lck

Equal amounts (25 µg) of protein from each time point were diluted 1:4 with 5X SDS-PAGE gel loading buffer (0.25M Tris-HCl, pH 6.8; 15% SDS; 50% glycerol; 25% β-mercaptoethanol; 0.01% bromophenol blue) and incubated at 95 ^{o}C for 10 min. Sample separation was performed by sodium dodecyl sulfate polyacrylamide gel electrophoresis (SDS-PAGE). Protein transfer was carried out using the iBlot Gel Transfer Device (Invitrogen) following the manufacturer instructions. The membrane was blocked for 1 h in blocking buffer (TBS/Tween-20/5% milk) at 20 ^{o}C and then incubated overnight at 4 °C with 1:3000 dilution of Lck monoclonal antibody (#MA1-19197, Thermo Fisher Scientific, Rockford, IL, USA). The membrane was washed 3×5 min at 20 ºC in TBS/Tweeen-20 buffer before incubating with the horseradish peroxidase (HRP)-conjugated IgG secondary antibody (#ab99697, Abcam) for 1 h at 20 ºC. Afterwards, the membrane was washed 3×10 min with TBS/Tween-20 and visualized by using the ECL method.

3. Results and discussion

3.1. Qualitative analysis of the Human Jurkat T cell phosphoproteome

In this study, we used human Jurkat T cells (JE6.1 and Jgamma1 clones) as a model to analyze the phosphorylation changes of human T cells upon costimulation with anti-CD3/anti-CD28 antibodies. The Jgamma1 clone is a PLC-γ-null T-cell which was originally prepared by mutagenesis and clonal selection from Jurkat WT cells [32]. Jgamma1 shows no expression of PLC-γ which results in impaired Ca+ mobilization after TCR activation. Despite a small,

transient rise in Ca^{+2} was still produced probably due to the action of the PLC-γ2, a minor PLC isoform in T-cells, no N-FAT activation or interleukin 2 production was observed in this clone. Although some differences between the two cell clones studied could be due to possible unknown mutagenesis-induced alterations in Jgamma1, these two clones constitute an accepted model for the study of the effect of the lack of PLC-γ expression in T-cells [33-35].

Experiments involved 5 biological replicates performed on different days. For each replicate, aliquots of 2.5×10^7 cells were activated for 15, 30, 60, 120 and 1440 min with antibodies (Figure 1). Common time-courses used for T-cell activation in quantitative proteomics studies range from seconds to several minutes [8, 12, 15] and up to 60 min [10]. In order to get an insight on late phosphorylation events, and taking advantage of the capability of TMT labelling for monitoring of up to 6 samples in parallel, we extended the activation time range up to 1440 min. However, probably due to the lack of FBS in the culture media and the high density of cells required for the activation, 95% cells died after the longer incubation/activation time (as observed by trypan blue staining). In consequence, the corresponding analytical data was discarded and thus the 1440 min time point was not taken into consideration for the following discussion. For the analysis, eighty micrograms of protein from control and treated cells were digested and labeled with the corresponding TMT reagents. The pooled TMT-labelled samples were separated into 6 fractions by SCX chromatography and each fraction was subjected to phosphopeptide enrichment by sequential IMAC and TiO_2 chromatography [24]. The IMAC and TiO_2 phosphopeptide fractions were analyzed separately by nanoLC-MS^n. According to the database matching strategy described in Experimental and elsewhere [24, 25], hits detected from at least two search engines were considered as positive identifications.

On average, we identified 2212 and 2078 non-redundant phosphopeptides per biological replicate in JE6.1 and Jgamma1, respectively (Table S0). In total, we identified 5585 non-redundant phosphopeptides matching 2008 different phosphoproteins from both cell clones. Among them, the numbers of detected non-redundant phosphopeptides and phosphoproteins in JE6.1 are slightly higher than those in Jgamma1. Notably, 2732 phosphopeptides (48.9%) and 1317 proteins (65.6%) are common to both cell clones (Fig. 2A and 2B, full sets of phosphopeptides and phosphoproteins are provided in Supplemental Tables S1 and S2). Although MS-based large scale phosphoproteomics studies are able to identify thousands of phosphorylated peptides, confident site localization remains challenging. The confident localization of phosphorylation events on a given peptide can be evaluated using several scoring algorithms including Ascore [25, 28], MD-score [36], LuciPHOr [37] or PhosphoRS [38]. In the set of the identified phosphopeptides, 3189 and 2955 phosphopeptides containing high confidence P-sites according to the Q-Ascore algorithm were detected in JE6.1 and Jgamma1, respectively. By comparing with the

PhosphositePlus database [39], we identified 130 and 114 novel phosphopeptides containing only high confidence P-sites in JE6.1 and Jgamma1, respectively (Supplemental Table S3). Eleven of these sites in each clone had been annotated previously in other species, and other 9 and 7 sites in JE6.1 and Jgamma1, respectively, were annotated as predicted in the database but there was not experimental evidence in humans. More importantly, about 60 new phosphopeptides containing high confidence P-sites, and with unequivocal protein assignation (pointing each to a single protein), were discovered from each cell clone (63 in JE6.1 and 57 in Jgamma1). These phosphopeptides represent new high confidence P-sites on their corresponding proteins (Supplemental Table S2).

3.2. Effects of PLCγ1 in human T cell's phosphorylation dynamics

Upon TCR stimulation, PLCγ1 is activated by ITK and catalyzes the formation of IP3 and DAG from PIP2, initiating numerous cellular events including Ca^{2+}- and DAG-induced responses, cytoskeletal rearrangements, and integrin activation pathways [5, 6]. An abnormal PLCγ1 activity results in changes of constitutive cell signaling pathways, and has been described as a potential risk of cancer. Vaqué et al. [40] reported that the acquisition of somatic mutations in PLCγ1 and other essential genes for normal T cell differentiation may affect the proliferation and survival mechanisms in cutaneous T cell lymphomas (CTCL). Data from another study [41] indicated the role of PLC γ1-R707Q mutation in representing an alternative way of activation of kinase insert domain receptor (KDR)/PLCγ1 signaling in angiosarcomas. In T cell signaling, PLCγ1 is central on the TCR-dependent proximal signaling complex through interacting with SLP-76, Vav1 and LAT [3, 5, 6]. To date, the effects of PLCγ1 on the T cell phosphoproteome is still poorly understood.

The present work introduces for the first time the phosphoproteome of Jgamma1 and the effect of PLCγ1 on phosphorylation dynamics of human T cells. For this purpose we analyzed the phosphorylation state of JE6.1 (wild type) and Jgamma1 (PLCγ1 null) upon CD3/CD28 costimulation at different time points (15, 30, 60, and 120 min). Cell activation was verified by Western blot analysis of two proteins involved in TCR signaling: the ribosomal protein S6 and the extracellular signal-regulated kinase 1/2 (ERK 1/2) (data not shown).

Overall, we identified 378 phosphopeptides (matched to 332 phosphoproteins) containing regulated P-sites in JE6.1, whereas only 71 phosphopeptides (matched to 71 phosphoproteins) containing regulated P-sites were detected in Jgamma1 (Supplemental Table S4 and S5). Several kinases were identified in the set of regulated proteins (18 and 3 in JE6.1 and Jgamma1 clones, respectively, Supplemental Tables S6). Significant phosphorylation changes were observed in cyclin-dependent kinases 1, 11B, 12 and 13 in JE6.1 clone. The lower number of phosphoproteins and

phosphopeptides containing regulated P-sites after TCR stimulation in the case of Jgamma1 probably reflects the vital role of PLCγ1 on TCR-driven signal transduction. Among the phosphopeptides containing regulated P-sites, 21 phosphopeptides (matched to 27 phosphoproteins) were common to both cell clones (Fig. 2C). The amino acid distribution (S/T/Y) of regulated P-sites was similar to that observed from non-regulated P-sites in both cell clones. Detectability of phosphorylation changes depends both in the detectability of the phosphopeptide (determined by the size, physicochemical characteristics, concentration of the tryptic sequence bearing the modification and the existence of possible co-eluting interferences) and the production of quantitative data of enough precision to reveal small changes that can be physiologically relevant. The observation window provided by shotgun approaches is being widened by the advances in the mass resolution and scan speed of modern MS instruments as well as by the development of more precise quantitative strategies [42]. Still, due to the inherent characteristics of the data-dependent shotgun approach, the number of sites reported here are doubtless only a fraction of the sites undergoing modification after TCR-activation.

3.3. Motif analysis of regulated phosphopeptides

Motif-X analysis of the high confidence phosphopeptide sets in our collections revealed the presence of several kinase substrate motifs including proline-directed, basophilic, and CK2 motifs in both cell types (Figure S2). The most frequent motif was the proline directed motif (xxxsPxx), specific for extracellular signal-regulated kinases 1 and 2 (ERK1/2), glycogen synthase kinase 3 (GSK-3) and cyclin-dependent-like kinase 5 (CDK-5) [30, 43]. This motif was also the most abundant in the collections of regulated P-sites from both clones. The second most frequent motif in the full collection was a basophilic CaMK2 motif (RxxSxxx) which was also very frequent in the sets of regulated phosphopeptides. These proline-directed and basophilic motifs have been reported to be regulated in human Primary T cells after 5 min activation with anti-CD3 antibodies [44]. The most specific motif (extracted in the first iteration of the Motif-X analysis) appearing in the full phosphosite collection (RxxsPxxx) has been recently described as specific for SR protein kinases [45], a family of proteins involved in RNA splicing. Interestingly, this motif did not appear when only the set of regulated phosphopeptides were considered in the Motif-X analysis, suggesting that the corresponding kinases are not playing a major role during cell activation. Similar profiles of proline-directed (xxxSPxx), basophilic (RRxxSxxxx and RxxSxxx), and CK2 (xxxSDxE and xxxSxxE) motifs were observed in JE6.1 when considering only the set of high confidence up-regulated phosphopeptides. In the case of Jgamma1, the proline directed motif is also observed among the up-regulated phosphopeptides although the motif with a higher score is a RxxxxSxxxxx motif which is present in 28% of the Jgamma1 final unique target peptides accepted by Motif-X. This motif has been reported as a partial motif for Akt kinase (canonical substrate motif RxRxxS/T) [46], a protein involved in cell

proliferation and survival through the PI3K/Akt signalling pathway and mTOR activation. The peptides bearing the RxxxxSxxxxx motifs pointed to 9 different proteins, including proteins related with T-Cell activation such as Lck (Ser-94) and DOCK2 (Ser-1705). As the number of upregulated phosphopeptides available for Motifs-X analysis was relatively low, confirmation of the differential presence of this motif on Jgamma1 would require further studies

3.4. Phosphoproteins containing regulated P-sites

Proteins containing regulated P-sites in JE6.1 were mapped into 13 different functional KEGG pathways by using DAVID analysis (Fig.3, p value < 0.05) [31]. Involved pathways, as those of the spliceosome, mitogen-activated protein kinase (MAPK), TCR signaling, and actin and cytoskeleton regulation reflect the well-known activities occurring during T cell activation [5, 6]. In Jgamma1, regulated P-sites-containing proteins map only to the spliceosome pathway, the gap junction pathway and other two KEGG pathways not related with cell activation (pathogenic *E.coli* infection and systemic lupus erythematosus). The difference on the represented pathways between JE6.1 and Jgamma1 could be explained by the negative influence of PLCγ1 deficiency on phosphorylation of TCR-responsive proteins. In contrast, we observed in both cell clones several common downstream PLCγ1 proteins containing up-regulated P-sites which are known to be related with TCR stimulation such as tubulins alpha-1B chain (TUBA1B), beta-4A chain (TUBB4A) and beta chain (TUBB). Mayya et al. [10] found that TCR stimulation by OKT3 lead to phosphorylation changes of multiple isoforms of tubulin and described the role of this phosphorylation in microtubule polarization. The phosphorylation changes of these downstream PLCγ1 proteins may suggest the existence of PLCγ1 independent pathways in response to CD3/CD28 costimulation of T cells.

Another protein related with microtubule polarization in our collection was stathmin. It has been described that phosphorylation of this protein on serine-25 and serine-38 abrogates its binding to microtubules contributing to their stabilization [10]. We found stathmin peptides phosphorylated on serine-16, serine-25 and serine-38. Serine-38 showed a significant, small increase at 30 min in JE.1 but none of the monophosphorylated peptides containing serine-16 or serine-25 showed a significant change after activation. Interestingly, the doubly phosphorylated peptide at serine-16 and serine-25 showed a significant up-regulation at all activation times in JE.1, especially at 15 and 30 min, suggesting a possible role of serine-16 in the activities assigned to serine-25. Contrarily to that observed in JE.1, this di-phosphorylated peptide was found down-regulated in Jgamma1 as well as the peptide phosphorylated at serine-25. None of the other two monophosphorylated peptides was detected in this clone. These results indicate the need of an unaltered pathway for stathmin phosphorylation at these sites.

Spliceosomal proteins make up the largest group in both cell clones (Figure 3). Phosphorylation and dephosphorylation of these proteins have been found to modulate protein–protein and protein–RNA interactions [47]. Shi et al. [48] suggested that changes in proteins such as SF3b155 and U5-116K could modulate the rearrangement of the spliceosome structure at the initial step of splicing. On the other hand, phosphorylation of several other spliceosomal proteins such as Prp6, Prp31, and hPrp28 is essential for the formation of the spliceosomal B-complex [49, 50]. These phosphorylation/dephosphorylation events trigger the critical nuclear ribonucleoprotein (RNP) rearrangement, thereby allowing the spliceosome machinery to function [51]. Mayya [10] detected changes in phosphorylation of 5 SR family proteins and 7 spliceosomal proteins after treatment with OKT3. Our work presents 16 and 9 proteins with phosphorylation changes in JE6.1 and Jgamma1, respectively, after T cell costimulation with anti-CD3/anti-CD28 antibodies. These findings may support the proposition from Mayya that phosphorylation seems to play a role in splicing of mRNAs after TCR stimulation.

We detected 33 phosphoproteins (from 27 protein nodes) and 26 phosphoproteins (from 22 protein nodes) from the KEGG-TCR signaling pathway in JE6.1 and Jgamma1, respectively; of them, 8 proteins showed significant phosphorylation changes upon CD3/CD28 costimulation in JE6.1, whereas only 1 protein (Lck) containing regulated P-sites was found out in Jgamma1 (Fig. 4). Notably, the only protein containing regulated P-sites (Lck) found in Jgamma1 is located upstream of PLCγ1 in the TCR signaling pathway, while no proteins with regulated P-sites were found downstream. Clearly, there is no significant difference in the number of phosphoproteins assigned to the KEGG-TCR signaling pathway between JE6.1 and Jgamma1. However, the number of proteins for which we detected regulated phosphopeptides in JE6.1 is remarkably higher than in Jgamma1. Thus, the absence of PLCγ1 seems to affect more the protein phosphorylation dynamics than the phosphorylation state in Jurkat T cells stimulated with anti-CD3/anti-CD28 antibodies.

3.5. Phosphorylation of Lck

Lck - a typical member of the SRC family kinase is one of the first molecules to be activated following TCR stimulation. Upon antigen recognition by the TCR complex, Lck molecules are attracted towards the TCR and phosphorylate tyrosine residues within the immunoreceptor tyrosine-based activation motifs (ITAM) of the cytoplasmic tails of the TCR-gamma chains and CD3 subunits, thereby initiating the TCR/CD3-dependent signaling pathways (reviewed in [5, 52]). Many P-sites from Lck have been identified, of which tyrosine-394 and tyrosine-505 is among the most important. The enzymatic activity of Lck is increased by the autophosphorylation on tyrosine-394 and

decreased by the phosphorylation on tyrosine-505 by C-terminal Src kinase (CSK) [53, 54]. In this work, we detected 14 P-sites on Lck from both cell clones; 13 of them are high confidence based on the Q-Ascore algorithm (Table 1). Prominently, besides the previously described P-sites, we detected four high confidence P-sites on Lck for which there was no experimental evidence for humans in PhosphositePlus database: serine-150, serine-377, serine-121, and serine-94. Phosphorylated serine-94, a site characterized in mouse in the database, was detected to be up-regulated only in the case of the Jgamma1 clone while serine-121 was found significantly increased in both clones after stimulation. The serine-121 phosphorylation level was observed to gradually increase over time although changes were higher in the case of JE6.1 (Figure 5A). This suggests that this phosphorylation is not related with the role of this protein in the initial events of TCR-triggered signaling occurring through the protein complexes in the membrane. In addition, and despite Lck is a protein typically acting upstream of PLC, the increase in serine-121 phosphorylation was very minor in the Jgamma1 clone, indicating that PLC or other downstream kinases could be involved in the process. Recently the translocation of Lck to the nucleus of primary and Jurkat T cell lines has been described, where it would act as a transcription factor [55, 56]. It has been shown that this translocation requires phosphorylation of tyrosine-394 which is in turn induced by TCR activation. Thus, the observed Lck phosphorylation at serine-121 could be related with this nuclear role and late events in response to TCR activation such as cell proliferation and for which functional PLC-γ is required.

Due to the potential interest of this finding, we further validated the characterization of the site and the characteristics of the observed changes. As mentioned above, the localization of P-sites on peptides could be validated by several scoring algorithms. However, the localization of P-sites on a protein is not always obtained due to the issue of shared peptides between multiple proteins. For example, in our collection, about half of the identified phosphopeptides from each cell clone (53.8% in JE6.1 and 53.9% in Jgamma1) could be assigned to 2 or more proteins. In the case of Lck, serine-121 was unambiguously identified by the same phosphopeptide in both cell clones (there is only one potential phosphorylation site in the peptide). A BLAST search against the Uniprot database (http://www.uniprot.org/) showed that this phosphopeptide might belong to several isoforms of Lck in addition to a few proteins of low experimental evidence. Besides the main Lck isoform (P06239), the peptide also matched to isoforms 2 and 3 of the protein. In all cases the P-site was located at position 121 of the protein. This indicated that phosphorylation changes observed in this phosphopeptide probably reflect changes on the corresponding Lck sequence. These changes were due to a higher proportion of phosphorylated versus non phosphorylated protein as indicated by Western blot experiments that showed no significant changes on the levels of total Lck over time (Figure 5B). To our knowledge, this is the first

evidence of phosphorylation at Serine-121 on Lck, a novel P-site regulated as a late response to TCR costimulation with anti-CD3/anti-CD28 antibodies.

4. Conclusions

We are reporting more than one hundred Jurkat phosphopeptides (130 and 114 peptides in the JE6.1 and Jgamma1 clones, respectively), from a collection of more than 2000 proteins, which were not previously described in the PhosphositePlus database, probably the most comprehensive collection of phosphosites available.

Quantitative analysis showed a remarkably lower number of phosphopeptides containing regulated P-sites in the Jgamma1 clone (71 phosphopeptides) compared to that in the JE6.1 clone (378 phosphopeptides), reflecting the vital role of PLCγ1 in T cell signaling.

We discovered 4 high confidence novel P-sites on Lck in response to CD3/CD28 costimulation, of which serine-121 showed significant changes in JE6.1 while only small changes in Jgamma1. These differences, together with the fact that Lck is a protein located upstream of PLCγ1 and that the observed phosphorylation takes place at long activation times, suggest that serine-121 phosphorylation could be involved in activities different to those occurring at the early stages of TCR-activation through the plasma membrane complexes. Further studies would be required to ascertain whether this late phosphorylation event is related with the nuclear roles previously described for the protein.

Acknowledgments: This work was carried out at LP-CSIC/UAB and supported by project BIO2013-46492-R from MINECO and VAST-CSIC bilateral action (2012VN0003). The CSIC/UAB Proteomics Laboratory of IIBB-CSIC is a member of Proteored, PRB2-ISCIII and is supported by grant PT13/0001, of the PE I+D+i 2013-2016, funded by ISCIII and FEDER.

REFERENCES

[1] Huse M. The T-cell-receptor signaling network. J Cell Sci. 2009;122:1269-73.

[2] Kane LP, Lin J, Weiss A. Signal transduction by the TCR for antigen. Curr Opin Immunol. 2000;12:242-9.

[3] Beach D, Gonen R, Bogin Y, Reischl IG, Yablonski D. Dual role of SLP-76 in mediating T cell receptor-induced activation of phospholipase C-gamma1. J Biol Chem. 2007;282:2937-46.

[4] Koretzky GA, Abtahian F, Silverman MA. SLP76 and SLP65: complex regulation of signalling in lymphocytes and beyond. Nat Rev Immunol. 2006;6:67-78.

[5] Brownlie RJ, Zamoyska R. T cell receptor signalling networks: branched, diversified and bounded. Nat Rev Immunol. 2013;13:257-69.

[6] Smith-Garvin JE, Koretzky GA, Jordan MS. T cell activation. Annu Rev Immunol. 2009;27:591-619.

[7] Plavec I, Sirenko O, Privat S, Wang Y, Dajee M, Melrose J, et al. Method for analyzing signaling networks in complex cellular systems. Proc Natl Acad Sci USA. 2004;101:1223-8.

[8] Cao L, Ding Y, Hung N, Yu K, Ritz A, Raphael BJ, et al. Quantitative phosphoproteomics reveals SLP-76 dependent regulation of PAG and Src family kinases in T cells. PLoS ONE. 2012;7:e46725.

[9] Kim J-E, White FM. Quantitative analysis of phosphotyrosine signaling networks triggered by CD3 and CD28 costimulation in Jurkat cells. J Immunol. 2006;176:2833-43.

[10] Mayya V, Lundgren DH, Hwang S-I, Rezaul K, Wu L, Eng JK, et al. Quantitative phosphoproteomic analysis of T cell receptor signaling reveals system-wide modulation of protein-protein interactions. Sci Signal. 2009;2:ra46.

[11] Navarro MN, Goebel J, Hukelmann JL, Cantrell DA. Quantitative phosphoproteomics of cytotoxic T cells to reveal protein kinase d 2 regulated networks. Mol Cell Proteomics. 2014;13:3544-57.

[12] Nguyen V, Cao L, Lin JT, Hung N, Ritz A, Yu K, et al. A new approach for quantitative phosphoproteomic dissection of signaling pathways applied to T cell receptor activation. Molecular & cellular proteomics. 2009;8:2418-31.

[13] Abraham RT, Weiss A. Jurkat T cells and development of the T-cell receptor signalling paradigm. Nat Rev Immunol. 2004;4:301-8.

[14] Jouy F, Müller SA, Wagner J, Otto W, von Bergen M, Tomm JM. Integration of conventional quantitative and phospho-proteomics reveals new elements in activated Jurkat T-cell receptor pathway maintenance. Proteomics. 2015;15:25-33.

[15] Salek M, McGowan S, Trudgian DC, Dushek O, de Wet B, Efstathiou G, et al. Quantitative phosphoproteome analysis unveils LAT as a modulator of CD3ζ and ZAP-70 tyrosine phosphorylation. PLoS ONE. 2013;8:e77423.

[16] Wiśniewski JR, Zougman A, Nagaraj N, Mann M. Universal sample preparation method for proteome analysis. Nat Methods. 2009;6:359-62.

[17] Carrascal M, Gay M, Ovelleiro D, Casas V, Gelpí E, Abian J. Characterization of the human plasma phosphoproteome using linear ion trap mass spectrometry and multiple search engines. J Proteome Res. 2010;9:876-84.

[18] Thingholm TE, Jensen ON, Robinson PJ, Larsen MR. SIMAC (sequential elution from IMAC), a phosphoproteomics strategy for the rapid separation of monophosphorylated from multiply phosphorylated peptides. Mol Cell Proteomics. 2008;7:661-71.

[19] Thingholm TE, Jorgensen TJ, Jensen ON, Larsen MR. Highly selective enrichment of phosphorylated peptides using titanium dioxide. Nat Protoc. 2006;1:1929-35.

[20] Dayon L, Pasquarello C, Hoogland C, Sanchez JC, Scherl A. Combining low- and high-energy tandem mass spectra for optimized peptide quantification with isobaric tags. J Proteomics. 2010;73:769-77.

[21] Eng JK, McCormack AL, Yates JR. An approach to correlate tandem mass spectral data of peptides with amino acid sequences in a protein database. J Am Soc Mass Spectrom. 1994;5:976-89.

[22] Geer LY, Markey SP, Kowalak JA, Wagner L, Xu M, Maynard DM, et al. Open mass spectrometry search algorithm. J Proteome Res. 2004;3:958-64.

[23] Gluck F, Hoogland C, Antinori P, Robin X, Nikitin F, Zufferey A, et al. EasyProt--an easy-to-use graphical platform for proteomics data analysis. J Proteomics. 2013;79:146-60.

[24] Carrascal M, Ovelleiro D, Casas V, Gay M, Abian J. Phosphorylation analysis of primary human T lymphocytes using sequential IMAC and titanium oxide enrichment. J Proteome Res. 2008;7:5167-76.

[25] Gallardo Ó, Ovelleiro D, Gay M, Carrascal M, Abian J. A collection of open source applications for mass spectrometry data mining. Proteomics. 2014;14:2275-9.

[26] Elias JE, Gygi SP. Target-decoy search strategy for increased confidence in large-scale protein identifications by mass spectrometry. Nat Methods. 2007;4:207-14.

[27] Vizcaino JA, Deutsch EW, Wang R, Csordas A, Reisinger F, Rios D, et al. ProteomeXchange provides globally coordinated proteomics data submission and dissemination. 2014;32:223-6.

[28] Beausoleil SA, Villén J, Gerber SA, Rush J, Gygi SP. A probability-based approach for high-throughput protein phosphorylation analysis and site localization. Nat Biotechnol. 2006;24:1285-92.

[29] Taverner T, Karpievitch YV, Polpitiya AD, Brown JN, Dabney AR, Anderson GA, et al. DanteR: an extensible R-based tool for quantitative analysis of -omics data. Bioinformatics. 2012;28:2404-6.

[30] Schwartz D, Gygi SP. An iterative statistical approach to the identification of protein phosphorylation motifs from large-scale data sets. Nat Biotechnol. 2005;23:1391-8.

[31] Huang DW, Sherman BT, Lempicki RA. Systematic and integrative analysis of large gene lists using DAVID bioinformatics resources. Nat Protoc. 2009;4:44-57.

[32] Irvin BJ, Williams BL, Nilson AE, Maynor HO, Abraham RT. Pleiotropic contributions of phospholipase C-gamma1 (PLC-gamma1) to T-cell antigen receptor-mediated signaling: reconstitution studies of a PLC-gamma1-deficient Jurkat T-cell line. Mol Cell Biol. 2000;20:9149-61.

[33] Balasubramanian S, Ramos J, Luo W, Sirisawad M, Verner E, Buggy JJ. A novel histone deacetylase 8 (HDAC8)-specific inhibitor PCI-34051 induces apoptosis in T-cell lymphomas. Leukemia. 2008;22:1026-34.

[34] Kremer KN, Clift IC, Miamen AG, Bamidele AO, Qian N-X, Humphreys TD, et al. Stromal cell-derived factor-1 signaling via the CXCR4-TCR heterodimer requires phospholipase C-β3 and phospholipase C-γ1 for distinct cellular responses. J Immunol. 2011;187:1440-7.

[35] Stoevesandt O, Köhler K, Wolf S, André T, Hummel W, Brock R. A network analysis of changes in molecular interactions in cellular signaling. Mol Cell Proteomics. 2007;6:503-13.

[36] Savitski MM, Lemeer S, Boesche M, Lang M, Mathieson T, Bantscheff M, et al. Confident phosphorylation site localization using the Mascot Delta Score. Mol Cell Proteomics. 2011;10:M110.003830.

[37] Fermin D, Walmsley SJ, Gingras A-C, Choi H, Nesvizhskii AI. LuciPHOr: algorithm for phosphorylation site localization with false localization rate estimation using modified target-decoy approach. Mol Cell Proteomics. 2013;12:3409-19.

[38] Taus T, Köcher T, Pichler P, Paschke C, Schmidt A, Henrich C, et al. Universal and confident phosphorylation site localization using phosphoRS. J Proteome Res. 2011;10:5354-62.

[39] Hornbeck PV, Kornhauser JM, Tkachev S, Zhang B, Skrzypek E, Murray B, et al. PhosphoSitePlus: a comprehensive resource for investigating the structure and function of experimentally determined post-translational modifications in man and mouse. Nucleic Acids Res. 2012;40:D261-70.

[40] Vaqué JP, Gómez-López G, Monsálvez V, Varela I, Martínez N, Pérez C, et al. PLCG1 mutations in cutaneous T-cell lymphomas. Blood. 2014;123:2034-43.

[41] Kunze K, Spieker T, Gamerdinger U, Nau K, Berger J, Dreyer T, et al. A recurrent activating PLCG1 mutation in cardiac angiosarcomas increases apoptosis resistance and invasiveness of endothelial cells. Cancer Res. 2014;74:6173-83.

[42] Erickson BK, Jedrychowski MP, McAlister GC, Everley RA, Kunz R, Gygi SP. Evaluating multiplexed quantitative phosphopeptide analysis on a hybrid quadrupole mass filter/linear ion trap/orbitrap mass spectrometer. Analytical chemistry. 2015;87:1241-9.

[43] Amanchy R, Periaswamy B, Mathivanan S, Reddy R, Tattikota SG, Pandey A. A curated compendium of phosphorylation motifs. Nat Biotechnol. 2007;25:285-6.

[44] Ruperez P, Gago-Martinez A, Burlingame AL, Oses-Prieto JA. Quantitative phosphoproteomic analysis reveals a role for serine and threonine kinases in the cytoskeletal reorganization in early T cell receptor activation in human primary T cells. Mol Cell Proteomics. 2012;11:171-86.

[45] Lipp JJ, Marvin MC, Shokat KM, Guthrie C. SR protein kinases promote splicing of nonconsensus introns. Nat Struct Mol Biol. 2015;22:611-7.

[46] Sutherland BW, Kucab J, Wu J, Lee C, Cheang MCU, Yorida E, et al. Akt phosphorylates the Y-box binding protein 1 at Ser102 located in the cold shock domain and affects the anchorage-independent growth of breast cancer cells. Oncogene. 2005;24:4281-92.

[47] Xiao SH, Manley JL. Phosphorylation of the ASF/SF2 RS domain affects both protein-protein and protein-RNA interactions and is necessary for splicing. Genes Dev. 1997;11:334-44.

[48] Shi Y, Reddy B, Manley JL. PP1/PP2A phosphatases are required for the second step of Pre-mRNA splicing and target specific snRNP proteins. Mol Cell. 2006;23:819-29.

[49] Mathew R, Hartmuth K, Möhlmann S, Urlaub H, Ficner R, Lührmann R. Phosphorylation of human PRP28 by SRPK2 is required for integration of the U4/U6-U5 tri-snRNP into the spliceosome. Nat Struct Mol Biol. 2008;15:435-43.

[50] Schneider M, Hsiao H-H, Will CL, Giet R, Urlaub H, Lührmann R. Human PRP4 kinase is required for stable tri-snRNP association during spliceosomal B complex formation. Nat Struct Mol Biol. 2010;17:216-21.

[51] Will CL, Lührmann R. Spliceosome structure and function. Cold Spring Harb Perspect Biol. 2011;3.

[52] Palacios EH, Weiss A. Function of the Src-family kinases, Lck and Fyn, in T-cell development and activation. Oncogene. 2004;23:7990-8000.

[53] Bergman M, Mustelin T, Oetken C, Partanen J, Flint NA, Amrein KE, et al. The human p50csk tyrosine kinase phosphorylates p56lck at Tyr-505 and down regulates its catalytic activity. EMBO J. 1992;11:2919-24.

[54] Bougeret C, Delaunay T, Romero F, Jullien P, Sabe H, Hanafusa H, et al. Detection of a physical and functional interaction between Csk and Lck which involves the SH2 domain of Csk and is mediated by autophosphorylation of Lck on tyrosine 394. J Biol Chem. 1996;271:7465-72.

[55] Ahmed Z, Beeton CA, Williams MA, Clements D, Baldari CT, Ladbury JE. Distinct spatial and temporal distribution of ZAP70 and Lck following stimulation of interferon and T-cell receptors. Journal of molecular biology. 2005;353:1001-10.

[56] Vahedi S, Chueh FY, Dutta S, Chandran B, Yu CL. Nuclear lymphocyte-specific protein tyrosine kinase and its interaction with CR6-interacting factor 1 promote the survival of human leukemic T cells. Oncology reports. 2015;34:43-50.

TABLES

Table 1. P-sites of Lck detected in the JE6.1 and Jgamma1 cell clones.

FIGURES

Figure 1. Jurkat T cells were activated with anti CD3/CD28 antibodies. Protein extracts were digested and labeled with the corresponding TMT reagents and the pooled material separated into 6 fractions by SCX chromatography. Each fraction was subjected to sequential IMAC and TiO_2 chromatography and the resulting phosphopeptide fractions were analyzed separately by nanoLC-MS^n. The full study comprised five biological replicates.

Figure 2. Overview of the phosphopeptide and phosphoprotein sets identified in JE6.1 and Jgamma1 cell clones. A) Non-redundant phosphopeptides and B) phosphoproteins identified. C) Non redundant phosphopeptides containing P-sites which were found regulated upon TCR activation.

Figure 3. KEGG pathway mapping of proteins containing regulated P-sites. All pathways shown are overrepresented in JE6.1 ($p<0.05$) while only the spliceosome, pathogenic E.coli infection, gap junction and systemic lupus erythematosus pathways passed the filter for Jgamma1.

Figure 4. KEGG-TCR signaling pathway of phosphoproteins detected in the JE6.1 and Jgamma1 cell clones. The red-filled shapes represent proteins containing regulated P-sites.

Figure 5. Phosphorylation changes at Serine-121 of Lck measured by mass spectrometry across the time course (A) and total Lck protein expression by Western blot analysis (B). Stars indicate adjusted P-value <0.05.

Table 1. P-sites of LCK detected in the JE6.1 and Jgamma1 cell clones. New P-sites (not described in PhosphoSiteDB) are indicated in the PhosphoSiteDB column.

No	P-sites	Q-Ascore *		PhosphoSitePlus	Regulation**
		JE6	JGM		
1	Tyrosine-505	97.7	123.5	Yes	NC
2	Threonine-210	40	___	Yes	NQ
3	Serine-213	33.8	___	Yes	NQ
4	Serine-150	81.2	95.5	No	NC
5	Threonine-198	1000	___	Yes	NQ
6	Serine-377	42.9	14.2	No	NQ
7	Serine-121	1000	1000	No	Up-regulated, lightly on gamma1 strongly on JE.1
8	Threonine-159	6.1	___	Yes	NQ
9	Serine-162	17.7	___	Yes	NQ
10	Serine-94	1000	1000	No***	Up-regulated in Jgamma1
11	Tyrosine-394	___	28	Yes	NC
12	Threonine-395	___	1000	Yes	NC
13	Serine-194	___	1000	Yes	NC
14	Tyrosine-470	___	1000	Yes	Up-regulated in Jgamma1

* 1000, unambiguous P-site, only 1 phosphorylation target residue; —, non-detected.

** NC, no significant change; NQ, non-quantified,

*** described in rat

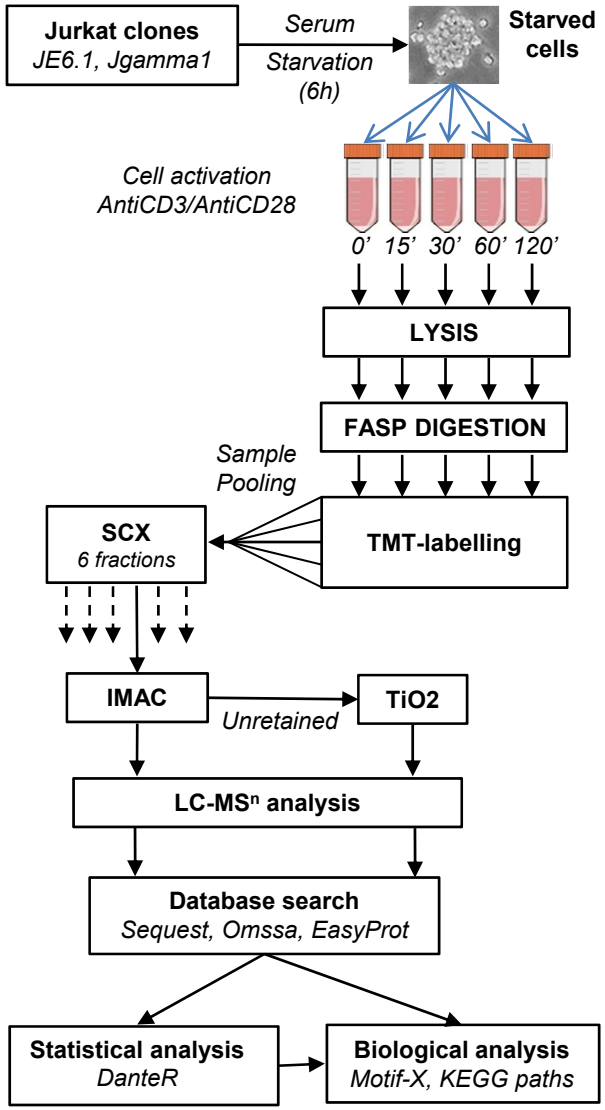
Jurkat clones
JE6.1, Jgamma1
Serum
Starvation
(6h)
Starved cells
Cell activation
AntiCD3/AntiCD28
0' 15' 30' 60' 120'
LYSIS
FASP DIGESTION
Sample
Pooling
SCX
6 fractions
TMT-labelling
IMAC
Unretained
TiO2
LC-MSn analysis
Database search
Sequest, Omssa, EasyProt
Statistical analysis
DanteR
Biological analysis
Motif-X, KEGG paths

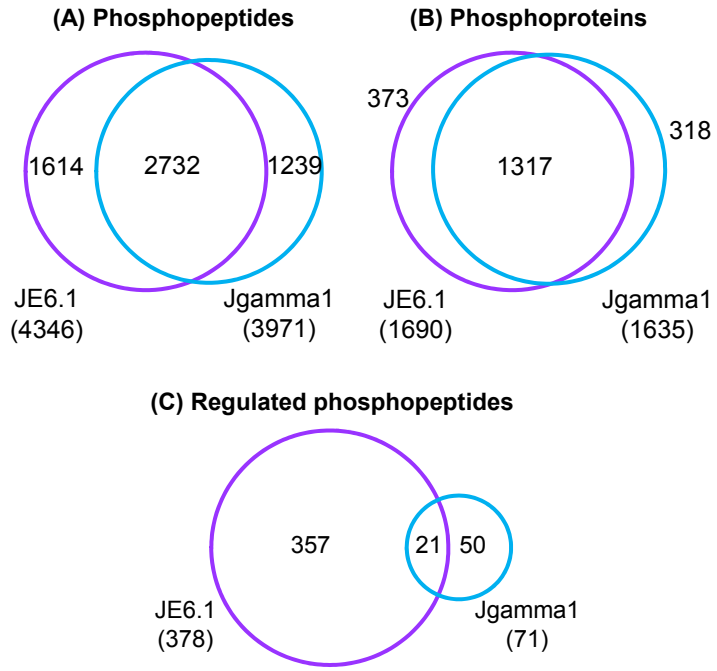
(A) Phosphopeptides
1614
2732
1239
JE6.1
(4346)
Jgamma1
(3971)
(B) Phosphoproteins
373
1317
318
JE6.1
(1690)
Jgamma1
(1635)
(C) Regulated phosphopeptides
357
21
50
JE6.1
(378)
Jgamma1
(71)

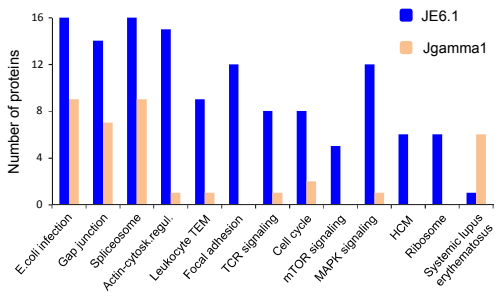
JE6.1
Jgamma1
Number of proteins
16
12
8
4
0
E.coli infection
Gap junction
Spliceosome
Actin-cytosk.regul.
Leukocyte TEM
Focal adhesion
TCR signaling
Cell cycle
mTOR signaling
MAPK signaling
HCM
Ribosome
Systemic lupus erythematosus

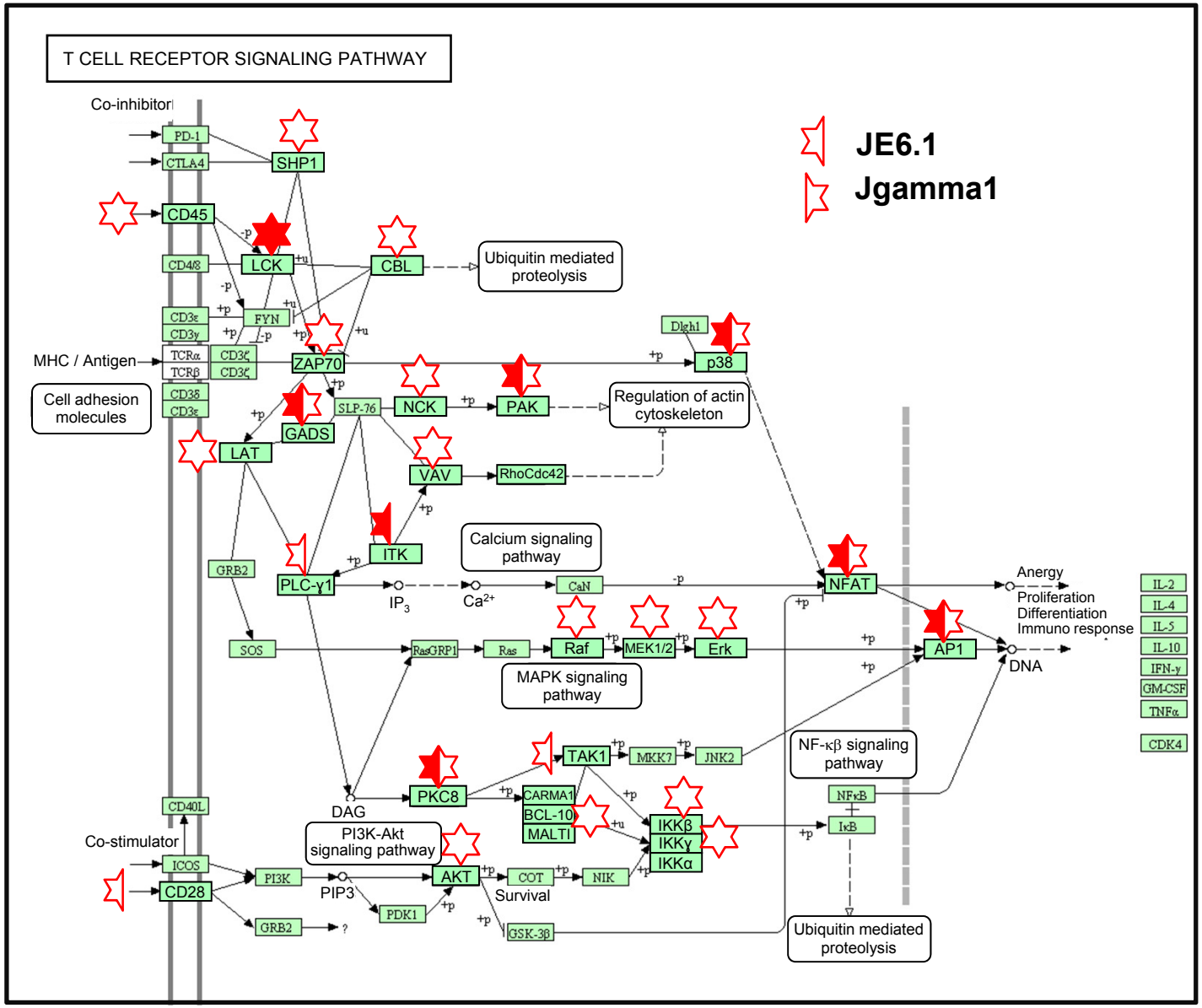
T CELL RECEPTOR SIGNALING PATHWAY
JE6.1
Jgamma1
Co-inhibitor
PD-1
CTLA4
SHP1
CD45
LCK
CBL
Ubiquitin mediated proteolysis
CD4/8
FYN
CD3ε
CD3γ
TCRα
TCRβ
CD3ζ
CD3ζ
ZAP70
MHC / Antigen
Cell adhesion molecules
CD3δ
CD3ε
Dlgh1
p38
SLP-76
NCK
PAK
Regulation of actin cytoskeleton
GADS
LAT
VAV
RhoCdc42
ITK
Calcium signaling pathway
GRB2
PLC-γ1
IP3
Ca2+
CaN
NFAT
Anergy
Proliferation
Differentiation
Immuno response
SOS
RasGRP1
Ras
Raf
MEK1/2
Erk
AP1
DNA
MAPK signaling pathway
IL-2
IL-4
IL-5
IL-10
IFN-γ
GM-CSF
TNFα
CDK4
TAK1
MKK7
JNK2
NF-κβ signaling pathway
PKC8
DAG
CARMA1
BCL-10
MALT1
IKKβ
IKKγ
IKKα
NFκB
IκB
CD40L
Co-stimulator
ICOS
CD28
PI3K
PIP3
PI3K-Akt signaling pathway
AKT
COT
NIK
Survival
PDK1
GRB2
GSK-3β
Ubiquitin mediated proteolysis

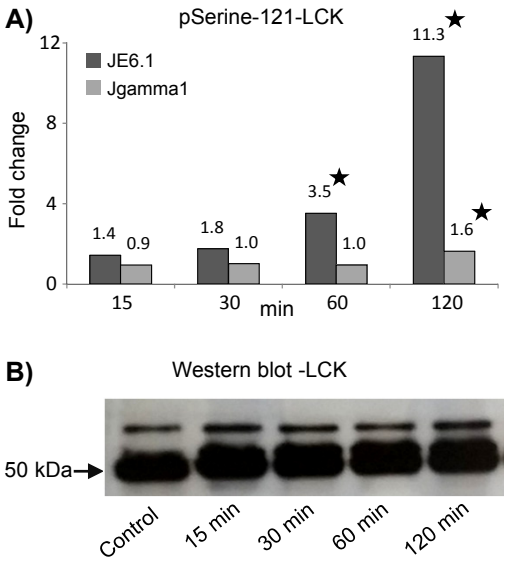
A)
pSerine-121-LCK
JE6.1
Jgamma1
Fold change
12
8
4
0
1.4
0.9
1.8
1.0
3.5
1.0
11.3
1.6
15
30
min
60
120
B)
Western blot -LCK
50 kDa
Control
15 min
30 min
60 min
120 min